

# A Variable-Temperature Solid-State $^{13}\text{C}$ CPMAS NMR Analysis of *meso*-Tetrapropylporphyrin and of Octaethylporphyrin

Lucio Frydman, Alejandro C. Olivieri, Luis E. Díaz, Aldonia Valasinas, and Benjamin Frydman\*

Contribution from the Facultad de Farmacia y Bioquímica, Universidad de Buenos Aires, Junin 956, Buenos Aires (1113), Argentina. Received November 9, 1987

**Abstract:** The high-resolution solid-state  $^{13}\text{C}$  NMR spectra of *meso*-tetrapropyl- and octaethylporphyrin were recorded with use of the CPMAS technique. Doublings in the pyrrole carbon signals of these compounds were ascribed to kinetic solid-state effects involved in the central hydrogen migration. It was found that whereas in *meso*-tetrapropylporphyrin the positions of the pyrrole carbon signals in the low temperature solution  $^{13}\text{C}$  NMR spectrum are similar to those in the room temperature solid-state NMR spectrum, this is not the case for octaethylporphyrin. In order to characterize the kinetic behavior of these compounds in the solid phase,  $^{13}\text{C}$  CPMAS NMR spectra were recorded at temperatures from slow to fast exchange limits. The changes observed in the spectra were analyzed assuming that the hydrogen migration proceeds between two tautomers of different energies. The shifts that are induced by the aromatic clouds of neighboring molecules were also calculated. With use of these ring current shifts and the low temperature solution chemical shift values, it was possible to obtain kinetic parameters of the solid-state reaction at different temperatures. The implications that the obtained results have for the understanding of the N-H tautomerization process in free base porphyrins are discussed, as well as the relevance that the latter may have for obtaining a mean structure of these compounds.

High-resolution  $^{13}\text{C}$  NMR studies in solution have afforded much information about the structural and electronic properties of organic molecules.<sup>1</sup> This technique, when performed at various temperatures, has been a major source of information concerning the kinetics and the thermodynamics of reactions in solution.<sup>2</sup> The cross-polarization (CP), high-power decoupling, magic-angle spinning (MAS) experiment<sup>3-5</sup> offers an extension of these isotropic chemical shift analyses to the solid state.<sup>6</sup> In general, the spectra obtained with this technique may differ from those obtained in solution both in the number of observed resonances as well as in their chemical shifts; and an understanding of these differences may retrieve important chemical information about the solid phase. When using the  $^{13}\text{C}$  CPMAS NMR technique to analyze the possibility of a chemical exchange process,<sup>7</sup> there are a number of factors that may prevent the clear understanding of the events taking place in the solid. The most evident one is the intrinsically lower resolution of the CPMAS experiment, as compared with solution NMR.<sup>8</sup> Other factors are related to the structure of the molecule under observation in the solid phase. For example, nuclei that are chemically equivalent in solution may become nonequivalent in the solid due to crystal packing effects.<sup>9</sup> An additional complication appears when some of the carbons being observed are attached to a  $^{14}\text{N}$ , since the dipolar coupling  $^{13}\text{C}$ - $^{14}\text{N}$  cannot be completely removed by MAS and the  $^{13}\text{C}$  resonances may appear broadened or split into an asymmetric doublet.<sup>10</sup>

Porphyrins are an interesting class of compounds, not only because of their great significance in biochemistry but also because of their peculiar electronic structure.<sup>11,12</sup> The large number of porphyrin derivatives that can be prepared offer the possibility of probing a wide range of physicochemical properties.<sup>13</sup> One of these properties, the tautomeric exchange of the inner hydrogens of free base porphyrins, has been the subject of numerous NMR studies in solution.<sup>14-21</sup> These studies have shown that in symmetrically substituted porphyrins, the central hydrogens can migrate from one pair of nitrogens to the other, giving rise to two tautomers **a** and **b** (Figure 1). The rate of the hydrogen migration was estimated by  $^1\text{H}$ ,  $^{13}\text{C}$ , and  $^{15}\text{N}$  variable-temperature NMR, and activation parameters could be obtained by fitting the data to the Arrhenius equation.<sup>15,16,19c,20,21</sup> Substitution of the central hydrogens by deuterons has also been performed in order to obtain the kinetic isotope effect, which was found to be unusually large.<sup>15,16,19</sup> All this experimental work has afforded considerable information about porphyrin tautomerism, although there is not yet enough experimental and theoretical evidence to establish unequivocally a mechanism for the reaction.

The tautomeric behavior of porphyrins has also been explored in the solid state. Such reaction is of possible technological interest since if a design could be achieved where the two states corresponding to the two proton positions are switched by an external method, the reaction could be used as a basis for information

(1) Abraham, R. J.; Loftus, P. *Proton and Carbon-13 NMR Spectroscopy*; Wiley: New York, 1985.

(2) Oki, M. *Applications of Dynamic NMR Spectroscopy to Organic Chemistry*; VCH Publishers: Deerfield Beach, FL, 1985.

(3) Pines, A.; Gibby, M. G.; Waugh, J. S. *J. Chem. Phys.* **1973**, *59*, 569.

(4) Schaeffer, J.; Stejskal, E. O. *J. Am. Chem. Soc.* **1976**, *98*, 1031.

(5) Andrew, E. R. *Progr. Nucl. Magn. Reson. Spectrosc.* **1971**, *8*, 1.

(6) (a) Fyfe, C. A. *Solid State NMR for Chemists*; C. F. C. Press: Ontario, 1983. (b) Yannoni, C. S. *Acc. Chem. Res.* **1982**, *15*, 201.

(7) Miller, R. D.; Yannoni, C. S. *J. Am. Chem. Soc.* **1980**, *102*, 7396.

(8) Shiau, W.-j.; Duesler, E. N.; Paul, I. C.; Curtin, D. Y.; Blaun, W. G.; Fyfe, C. A. *J. Am. Chem. Soc.* **1980**, *102*, 4546. Fyfe, C. A.; Lyerla, J. R.; Yannoni, C. S. *Acc. Chem. Res.* **1982**, *15*, 208.

(9) VanderHart, D. L.; Earl, W. L.; Garroway, A. N. *J. Magn. Reson.* **1981**, *44*, 361.

(10) (a) Lipmaa, E.; Alla, M. A.; Pehk, T. J.; Engelhart, G. *J. Am. Chem. Soc.* **1978**, *100*, 1929. (b) Scheffer, J. R.; Wong, Y.-F.; Patil, A. O.; Curtin, D. Y.; Paul, I. C. *J. Am. Chem. Soc.* **1985**, *107*, 4898.

(11) (a) Frey, M. H.; Opella, S. J. *J. Chem. Soc., Chem. Commun.* **1980**, 479. (b) Ballmann, G. E.; Groombridge, C. J.; Harris, R. K.; Packer, K. J.; Say, B. J.; Tanner, S. F. *Phil. Trans. R. Soc. London* **1981**, *A299*, 665.

(11) Dolphin, D., Ed. *The Porphyrins*; Academic: New York, 1979.

(12) Smith, K., Ed. *Porphyrins and Metalloporphyrins*; Elsevier: Amsterdam, 1975.

(13) Adler, A. D., Ed. *Ann. N.Y. Acad. Sci.* **1973**, 206.

(14) Storm, C. B.; Teklu, Y. *J. Am. Chem. Soc.* **1972**, *94*, 1745.

(15) Abraham, R. J.; Hawkes, G.; Smith, K. *Tetrahedron Lett.* **1974**, 1483.

(16) Eaton, S. S.; Eaton, G. R. *J. Am. Chem. Soc.* **1977**, *99*, 1601.

(17) Gust, D.; Roberts, J. D. *J. Am. Chem. Soc.* **1977**, *99*, 3637.

(18) Yeh, H. J. C.; Sato, M.; Morishima, I. *J. Magn. Reson.* **1977**, *26*, 365.

(19) (a) Limbach, H.-H.; Hennig, J. *J. Chem. Soc., Faraday Trans II* **1979**, *75*, 752. (b) Limbach, H.-H.; Hennig, J. *J. Chem. Phys.* **1979**, *71*, 3120.

(c) Limbach, H.-H.; Hennig, J.; Gerritzen, D.; Rumpel, H. *Faraday Discuss. Chem. Soc.* **1982**, *74*, 229. (d) Limbach, H.-H.; Hennig, J.; Stulz, J. *J. Chem. Phys.* **1983**, *78*, 5432. (e) Hennig, J.; Limbach, H.-H. *J. Am. Chem. Soc.* **1984**, *106*, 292.

(20) (a) Stilbs, P.; Moseley, M. E. *J. Chem. Soc., Faraday Trans. II* **1980**, *76*, 729. (b) Stilbs, P. *J. Magn. Reson.* **1984**, *58*, 152.

(21) (a) Crossley, M. J.; Harding, M. M.; Sternhell, S. *J. J. Am. Chem. Soc.* **1986**, *108*, 3608. (b) Crossley, M. J.; Field, L. D.; Harding, M. M.; Sternhell, S. *J. J. Am. Chem. Soc.* **1987**, *109*, 2335.

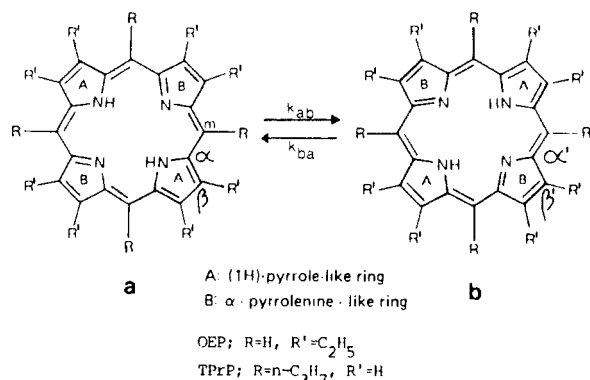


**Figure 1.** N-H tautomerism of *meso*-tetrapropylporphyrin (TPrP) and of octaethylporphyrin (OEP) showing the atoms labeling.

storage.<sup>22</sup> A variable-temperature <sup>15</sup>N CPMAS NMR analysis performed on isotopically enriched TPP and TTP<sup>23</sup> revealed that in the former tautomerism was influenced by the crystalline packing forces.<sup>24</sup> In a recent study<sup>25</sup> we reported the high-resolution solid-state <sup>13</sup>C NMR spectra of porphine and of four 5,10,15,20-tetraalkylporphyrins. By performing a variable-temperature analysis on porphine both in the solid state and in solution, we showed that the effects of crystal packing forces on the tautomeric behavior of this compound, if present, are very small. A similar conclusion was reached by Limbach and coworkers using <sup>15</sup>N CPMAS NMR.<sup>26</sup> On the other hand, all the tetraalkylporphyrins showed doublings of the pyrrole carbon resonances in their room temperature spectra. The doublings were assumed to reflect the perturbation of the process  $a \rightleftharpoons b$  (Figure 1) in the solid phase rather than inequivalencies within the asymmetric unit cell of otherwise chemically equivalent carbons. This assumption was based on the similarity between the magnitudes of the doublings in the  $\alpha$  and  $\beta$  carbon resonances in the solid-state spectra and in the low-temperature <sup>13</sup>C NMR spectrum of TPP. However, the experimental data were still insufficient to discern between a N-H tautomerization process slow on the NMR time scale and a fast migration taking place between two unequally populated tautomers. Doublings in the pyrrole carbon resonances were also found in the first solid state NMR analysis of free base porphyrins.<sup>27</sup> In this study, the <sup>13</sup>C CPMAS NMR spectra of OEP and its Zn(II) and Ni(II) complexes were recorded at room temperature, and the free base showed three resonances in the pyrrole region ( $\alpha$  and  $\beta$  carbons). This multiplicity was attributed to the presence of only one tautomer with diagonally situated hydrogens in solid-state OEP at room temperature, in accordance with the available X-ray data for this compound.<sup>28</sup>

In the present study, further information about the "topochemistry" of the hydrogen migration in solid free base porphyrins is presented. Attention is focused on two different model compounds which have already been analyzed by X-ray diffraction: TPrP and OEP.<sup>28,29</sup> The <sup>13</sup>C CPMAS NMR spectra of these compounds were recorded in the solid state and in solution at temperatures that ranged from the slow to the fast exchange limits. It was found that whereas in TPrP the tautomerism is just below coalescence at room temperature in the solid state, a fast hydrogen migration in OEP at this temperature takes place between two unequally populated tautomers. Rate and equilibrium

constants were obtained from the CPMAS NMR spectra and compared with those measured in solution. Other factors that influence the solid-state spectra, like the residual <sup>13</sup>C-<sup>14</sup>N coupling and the effects of the porphyrin diamagnetic ring currents, were also detected and were included in the analysis. Finally, we discuss the advantages and disadvantages of the solid-state NMR experiments over those in solution, as well as the way in which the former ones may help to understand the nature of porphyrin tautomerism.

## Experimental Section

Synthesis of TPrP was achieved by a modification of the Adler and Longo procedure.<sup>30</sup> Freshly distilled pyrrole (1.12 mL,  $8 \times 10^{-3}$  mol) and reagent grade butyraldehyde (1.60 mL,  $8 \times 10^{-3}$  mol) were added to 100 mL of propionic acid and heated under reflux. After boiling for 5 min, the solution was allowed to reach room temperature protected from light. The mixture was evaporated to dryness, and the solid residue was dissolved in a small volume of chloroform/hexane (3:1) and filtered through a TLC grade silica gel column ( $4 \times 20$  cm) with the same solvent as eluent. The fraction containing the purple product was evaporated to dryness and was crystallized from chloroform/methanol. For further purification, the porphyrin was dissolved in chloroform and filtered through a column ( $2 \times 20$  cm) of neutral alumina grade III. The fraction containing the porphyrin was evaporated in vacuo and crystallization from chloroform/methanol afforded 100 mg (2.8%) of pure TPrP. OEP was purchased from Porphyrin Products (Logan, Utah) and was used after crystallization from toluene.

The <sup>13</sup>C CPMAS NMR spectra were obtained on a highly modified XL-100-15 NMR spectrometer at 25.16-MHz <sup>13</sup>C and 100.06-MHz <sup>1</sup>H radio frequency fields. The probe is a single-coil double-tuned home-built system that uses a D<sub>2</sub>O external lock for field stabilization. The isolation between the proton and carbon channels is in excess of 50 db. A standard single-contact Hartmann-Hahn cross-polarization sequence was used<sup>31</sup> with <sup>1</sup>H and <sup>13</sup>C resonance radio frequency fields matched at approximately 80 kHz. The contact and delay time used were 3 ms and 3 s, respectively. A spin temperature inversion sequence that consists of a phase alternation in the initial  $\pi/2$  proton pulse and the receiver phase was used in order to minimize baseline distortions. The spinning apparatus used is a modified version of the Lowe design with a Macor stator and a boron nitride rotor that does not produce a <sup>13</sup>C background. The spinning frequencies varied between 3 and 5 kHz, high enough to completely remove unwanted spinning sidebands. The magic angle was adjusted by revolving the stator while monitoring the signal from a rotor containing a standard sample of hexamethylbenzene (HMB). The high-field signal of HMB (17.6 ppm) was used as external reference.

Variable-temperature operation was achieved by cooling or heating the driving and bearing gas, which was always air. Air was cooled in liquid nitrogen after being dried for the low-temperature operation and was heated by means of a resistance for the high-temperature operation. Temperature was regulated with a home-manufactured temperature controller and is considered accurate to  $\pm 2$  °C. All spectra were recorded with 30–80 mg of sample.

<sup>13</sup>C solution NMR spectra were obtained on Varian XL-400 and VXR-500 spectrometers at 100 and 125 MHz, respectively. Temperatures were calibrated after each run with use of the chemical shifts of CH<sub>3</sub>OH.<sup>32</sup> The concentration of solute used was about  $10^{-3}$  mol·L<sup>-1</sup> for OEP and  $2 \times 10^{-3}$  mol·L<sup>-1</sup> for TPrP in methylene-*d*<sub>2</sub> chloride. The chemical shifts were measured relative to CD<sub>2</sub>Cl<sub>2</sub> and then converted to the TMS scale.

## Results

**TPrP: Peak Assignments.** The room temperature high-resolution solid-state and solution <sup>13</sup>C NMR spectra of TPrP are shown in Figure 2, parts A and B, respectively. To assist the assignment of the solid-phase data, a spectrum was recorded employing the pulse sequence devised by Opella and Frey.<sup>33</sup> This routine allows one to obtain spectra that only show resonances from quaternary or methyl carbons by introducing a short delay (ca. 50  $\mu$ s) prior to the acquisition, during which the signals with stronger dipolar coupling to protons decay. The TPrP spectrum recorded under dipolar dephasing conditions is shown in Figure 2C, and only signals of quaternary carbons (e.g.,  $\alpha$  and meso carbons) and of

(22) Curtin, D. Y.; Paul, I. C. *Chem. Rev.* **1981**, *81*, 525.

(23) Abbreviations: TPP, *meso*-tetraphenylporphyrin; TTP, *meso*-tetra-*tert*-butylporphyrin; OEP, octaethylporphyrin; TPrP, *meso*-tetrapropylporphyrin; H<sub>2</sub>P, porphine.

(24) Limbach, H.-H.; Hennig, J.; Kendrick, R.; Yannoni, C. S. *J. Am. Chem. Soc.* **1984**, *106*, 4059.

(25) Frydman, L.; Olivieri, A. C.; Diaz, L. E.; Frydman, B.; Morin, F. G.; Mayne, C. L.; Grant, D. M.; Alder, A. D. *J. Am. Chem. Soc.* **1988**, *110*, 336.

(26) Wehrle, B.; Limbach, H.-H.; Koehler, M.; Ermer, O.; Vogel, E. *Angew. Chem.* **1987**, *26*, 934.

(27) Okazaki, M.; McDowell, C. A. *J. Am. Chem. Soc.* **1984**, *106*, 3185.

(28) Lauber, J. W.; Ibers, J. A. *J. Am. Chem. Soc.* **1973**, *95*, 5148.

(29) Codding, P. W.; Tulinsky, A. *J. Am. Chem. Soc.* **1972**, *94*, 4151.

(30) Adler, A. D.; Longo, F. R.; Finarelli, J. D.; Goldmacher, J.; Assour, J.; Korsakoff, L. *J. Org. Chem.* **1967**, *32*, 476.

(31) Hartmann, S. R.; Hahn, E. L. *Phys. Rev.* **1962**, *128*, 2042.

(32) Van Geet, A. L. *Anal. Chem.* **1968**, *40*, 2227.

(33) Opella, S. J.; Frey, M. H. *J. Am. Chem. Soc.* **1979**, *101*, 5855.

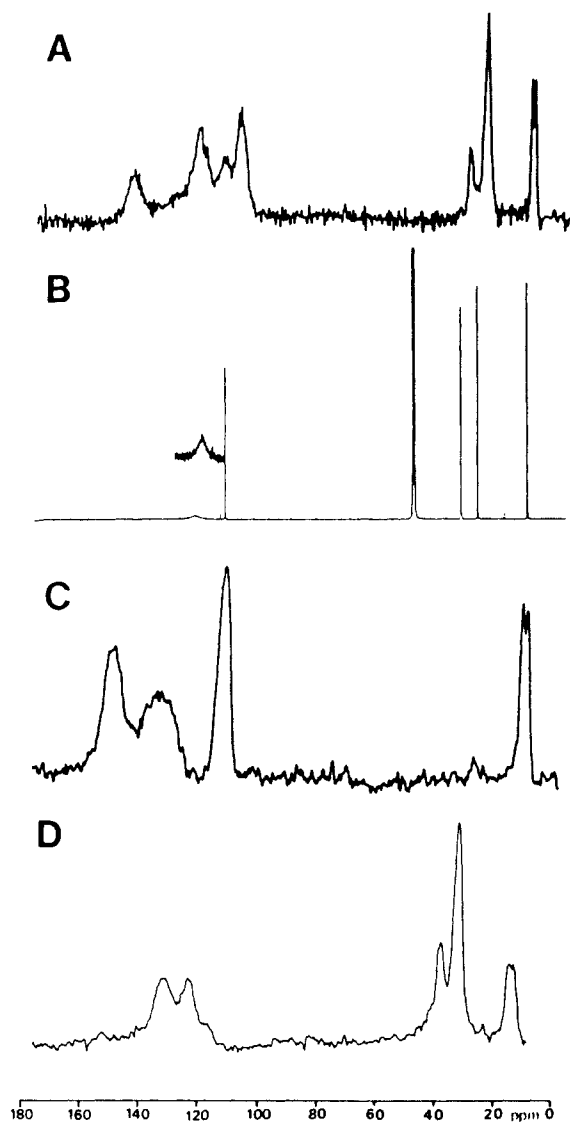


**Figure 2.** (A) High-resolution solid-state 25.16-MHz  $^{13}\text{C}$  NMR spectrum of TPrP recorded at room temperature. (B) Solution  $^{13}\text{C}$  NMR spectrum of TPrP recorded in a saturated solution of  $\text{CD}_2\text{Cl}_2$ . The inset shows the signals arising from the pyrrolic carbons. The spectrum was recorded at 125 MHz, 3700 transients, 26 500 Hz spectral width,  $54^\circ$  pulse angle. (C) Same as spectrum A but introducing a 50- $\mu\text{s}$  delay prior to the acquisition that allows only  $\text{CH}_3$  and quaternary carbons to appear. (D) Same as spectrum A but using a contact time of 40  $\mu\text{s}$  that allows mainly CH and  $\text{CH}_2$  residues to cross polarize. Spectral parameters for the solid-state spectra are the following: average number of scans = 30000, sweep width = 10000 Hz, Fourier number = 4096, line broadening = 10 Hz, repetition time = 2 s.

the  $\text{CH}_3$  groups appear. A spectrum consisting mainly of CH and  $\text{CH}_2$  can also be obtained by using a short (ca. 50  $\mu\text{s}$ ) contact time so that only carbons with strong dipolar coupling to protons (short  $T_{\text{CH}}$ ) are allowed to cross-polarize. This spectrum of TPrP is shown in Figure 2D, where the  $\beta$  and the  $\text{CH}_2$  carbons appear.

Although the room temperature solution and solid-state  $^{13}\text{C}$  NMR spectra of TPrP share some common general features, they possess a number of evident differences. Doublings appear in the CPMAS spectrum for the  $\alpha$  and the  $\beta$  carbon resonances, as well as for the signals of the methyl and meso carbons.<sup>34</sup> The methylene signals in the solid are also different from those appearing in the solution spectrum. While in the latter the two  $\text{CH}_2$  signals have similar heights indicating similar NOE's and  $T_1$ 's, in the CPMAS spectrum they show marked differences in their relative areas, even though it has been shown that quantitative

(34) The splitting in the meso carbon signal can be appreciated more clearly in the 50-MHz  $^{13}\text{C}$  CPMAS NMR spectrum of TPrP shown in ref 25.

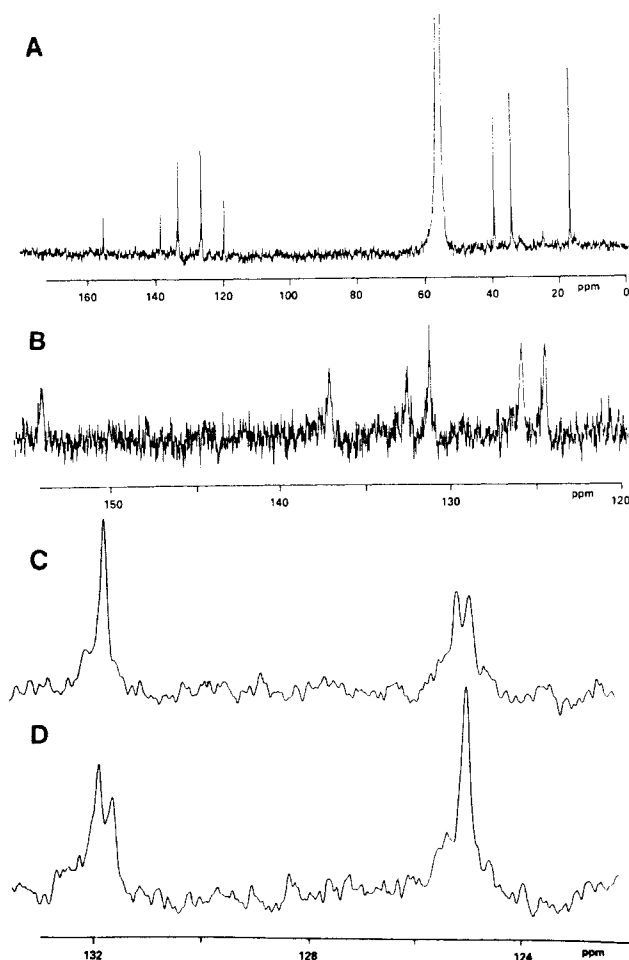


**Figure 3.** Low-temperature ( $-60^\circ\text{C}$ ) 125-MHz spectra of TPrP in  $\text{CD}_2\text{Cl}_2$ . (A) Proton decoupled spectrum, 3000 scans. (B) Proton coupled spectrum of the pyrrole region ( $\alpha$  and  $\beta$  carbons), 25000 scans. (C) Carbon spectrum recorded with single frequency decoupling at 9.49 ppm ( $\beta$  hydrogens of the  $\alpha$ -pyrroline like ring), 1000 scans. (D) Same as spectrum C, obtained by decoupling of the hydrogens appearing at 9.60 ppm.

reliability in the CPMAS spectra of protonated carbons is generally higher than that of  $^{13}\text{C}$  solution NMR.<sup>35</sup> This abnormality could reflect a difference in the cross-polarization rates of the two methylenes, although no difference in the relative areas of these peaks was observed upon changing the contact time. A more plausible explanation would be the splitting of the low-field methylene resonances into two peaks, one of which overlaps the methylene resonance at higher field giving rise to two signals with an area ratio of 1:3, a possibility that is further analyzed below.

The largest differences between the solid-state and the solution  $^{13}\text{C}$  NMR spectra appear in the pyrrole carbons region (118–155 ppm). In order to analyze the origin of these differences a study of the solution data was carried out. Little information is available from the room temperature spectrum (Figure 2B) since it only shows a single broad resonance around 128.7 ppm attributed to the  $\beta$  carbons, while the  $\alpha$  carbons signal does not appear at all. In order to explore the effects of the migration of the central hydrogens on these signals, a solution spectrum was registered at low temperature ( $-60^\circ\text{C}$ , Figure 3A). This spectrum shows four signals from the pyrrole carbons, and in order to differentiate the resonances from each group of carbons a proton coupled  $^{13}\text{C}$  NMR spectrum was recorded at low temperature (Figure 3B). As can be seen the resonances at 131.7 and 125.0 ppm are split with a  $J_{\text{CH}} = 180$  Hz and are therefore ascribed to the  $\beta$  carbons, while the  $\alpha$  carbons appear as small, unsplit peaks at 154.0 and 137.0 ppm.

(35) Alemany, L. B.; Grant, D. M.; Pugmire, R. J.; Alger, T. D.; Zilm, K. W. *J. Am. Chem. Soc.* **1983**, *105*, 2133.

**Table I.**  $^{13}\text{C}$  NMR Chemical Shifts of TPrP in the Solution and Solid-State Spectra

atom	chemical shift		
	solution (20 °C) <sup>a</sup>	solution (-60 °C) <sup>a</sup>	solid (30 °C) <sup>b</sup>
C <sub>α</sub> <sup>e</sup>	<i>c</i>	154.0	152.5
C <sub>α</sub> <sup>f</sup>	<i>c</i>	137.0	134.0
C <sub>β</sub> <sup>e</sup>	128.7 <sup>d</sup>	131.7	130.8
C <sub>β</sub> <sup>f</sup>		125.0	121.0
meso	118.7	118.2	116.7, 115.0
CH <sub>2</sub>	37.7, 32.1	37.2, 32.0	38.9, 33.2
CH <sub>3</sub>	15.1	14.9	15.3, 13.6

<sup>a</sup>In ppm downfield from TMS with CD<sub>2</sub>Cl<sub>2</sub> as solvent. <sup>b</sup>In ppm downfield from TMS with the CH<sub>3</sub> resonance of hexamethylbenzene as external reference. <sup>c</sup>Indistinguishable from baseline noise. <sup>d</sup>Broad signal. <sup>e</sup>Carbons in the  $\alpha$ -pyrroline-like ring (Figure 1). <sup>f</sup>Carbons in the (1*H*)-pyrrole-like ring.

Once the  $\alpha$  and  $\beta$  carbon resonances are identified, the question of how to assign the upfield and the downfield signals for each of these carbons remains. For the  $\alpha$  carbons, where the differences between the signals is ca. 17 ppm, an assignment may be proposed by comparison with model heterocycle compounds, such as pyridine and pyrrole. In the former the carbons bonded to the azine nitrogen ( $-\text{N}=\text{C}$ ) appear at 150.6 ppm whereas in the latter the carbons bonded to the imino nitrogen ( $-\text{NH}-$ ) appear at 118.5 ppm, suggesting that the downfield carbon resonance should be assigned to the  $\alpha$ -pyrroline-like ring and the high-field resonance to the (1*H*)-pyrrole-like ring (see Figure 1). In principle, a similar assignment could be proposed for the  $\beta$  carbon resonances, although this time the analogy is not as reliable as above. Not only is the difference between the  $\beta$  carbons (6.7 ppm) smaller than for the  $\alpha$  carbons, but also neither of the observed  $\beta$  resonances appear close to the chemical shift of the carbons  $\beta$  to the pyrrole nitrogen (108.2 ppm). Thus, in order to identify the origin of each  $\beta$  carbon signal selective decoupling experiments were carried out. When the proton NMR spectrum of TPrP is recorded at low temperature (i.e., below the coalescence temperature), the hydrogens bonded to the  $\beta$  carbons split into two peaks at 9.48 and 9.59 ppm. Although the areas of the two peaks are equal, the peak at lower field is broader due to an unresolved  $J^4$  coupling with the central hydrogens, indicating that it belongs to the  $\beta$  hydrogens in the (1*H*)-pyrrole-like ring. This was confirmed by irradiating the central hydrogens (at -2.9 ppm) and observing an equalization in the  $\beta$  hydrogen peak heights. Once the hydrogen resonances are assigned, it is possible to differentiate the  $\beta$  carbons by recording a  $^{13}\text{C}$  NMR spectrum using on resonance proton decoupling at -60 °C. This experiment is shown in Figure 3, spectra C and D, where it can be appreciated that irradiation of the protons at 9.49 ppm decouples the 131.7-ppm resonance while irradiation at 9.59 ppm decouples the peak at 125 ppm. Therefore, we assign the downfield signals of both the  $\alpha$  and the  $\beta$  carbons to the  $\alpha$ -pyrroline-like ring and the upfield ones to the (1*H*)-pyrrole-like ring.

We turn now to discuss the solid-state  $^{13}\text{C}$  NMR data. On the basis of the spectra shown in Figures 2, C and D, the peaks appearing at 152.5 and 134.0 ppm are assigned to two groups of chemically inequivalent  $\alpha$  carbons whereas the 121.0- and 130.8-ppm peaks are attributed to two groups of inequivalent  $\beta$  carbons. The similarity between the solid-state spectrum recorded at room temperature and the broadband  $^1\text{H}$  decoupled solution spectrum recorded in the slow exchange limit suggests that the doublings appearing in the former spectrum should be ascribed to effects that crystal packing forces exert on the N-H tautomerism in the solid phase, as adumbrated in our former work.<sup>25</sup> Solution and solid-state chemical shifts values are summarized in Table I, together with the corresponding assignments.

**OEP: Peak Assignments.** OEP is one of the most widely used model compounds for structural studies related to naturally occurring porphyrins. Therefore, although the 50-MHz  $^{13}\text{C}$  CPMAS NMR spectrum of OEP has already been reported,<sup>27</sup> it is profitable to revisit the problem with the aid of a variable-temperature

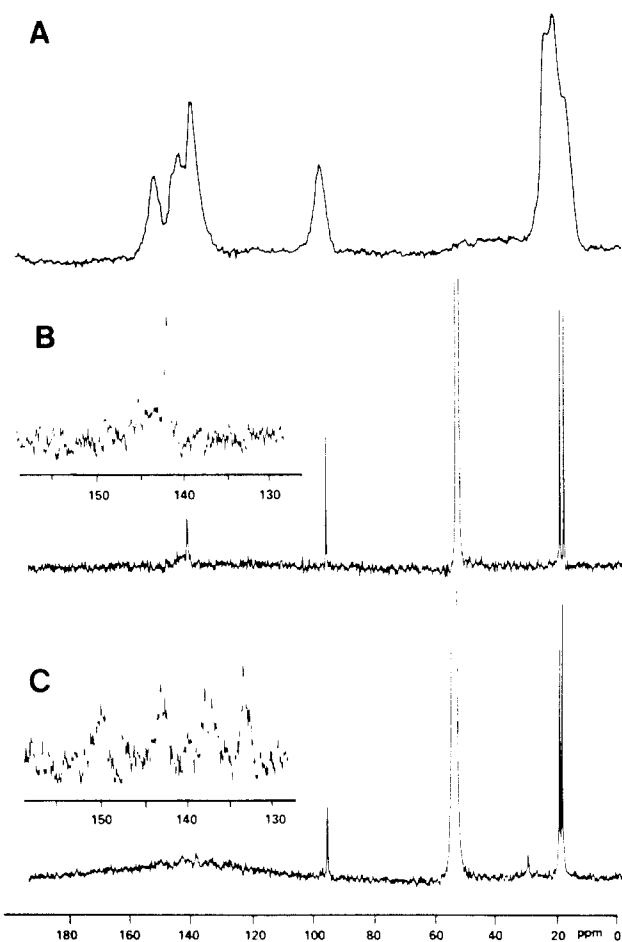


**Figure 4.** High-resolution solid-state (A) and solution (B, C)  $^{13}\text{C}$  NMR spectra of OEP. Solution spectra were recorded at 100 MHz with a saturated solution in CD<sub>2</sub>Cl<sub>2</sub>. Spectral parameters are the following: (A) 5000 scans, 10000 Hz spectral width, 3 s repetition time, temperature = 30 °C; (B) 512 scans, 20000 Hz spectral width, 5 Hz line broadening, temperature = 21 °C; (C) 4000 scans, temperature = -80 °C, other parameters are as in spectrum B.

analysis. The high-resolution solid-state and solution  $^{13}\text{C}$  NMR spectra of OEP recorded at room temperature are shown in Figure 4, A and B. In this case, the analysis of the pyrrole carbon resonances is more cumbersome than in the case of TPrP since all these carbons are quaternary, and the dipolar dephasing sequence does not introduce any simplification in the CPMAS spectrum. The solution spectrum of this zone is also poor, in part due to the absence of  $\beta$  hydrogens and in part due to the low solubility of OEP (ca.  $10^{-3}$  mol·L<sup>-1</sup>). Peak assignment of this spectrum is based on literature data: CH<sub>3</sub>,  $\delta$  = 18.45 ppm; CH<sub>2</sub>,  $\delta$  = 19.8 ppm; meso carbon,  $\delta$  = 96.5 ppm;  $\beta$  carbon,  $\delta$  = 141.5 ppm;  $\alpha$  carbon (broad),  $\delta$  = 144.0 ppm. As for TPrP, the N-H tautomerism affects the widths of the  $\alpha$  and of the  $\beta$  carbons, and the coalescence temperature of the former is close enough to room temperature so as to make them almost undetectable. On the basis of these solution chemical shifts the CPMAS spectrum was analyzed by assigning the broad peak at ca. 19 ppm to superimposed CH<sub>3</sub> and CH<sub>2</sub> resonances, the peak at 95 ppm to the meso carbon, and the triplet-like signal in the 135–150 ppm zone to the pyrrole carbons.<sup>27</sup> Unlike the solution spectrum, these carbons possess a signal intensity similar to the rest of the porphyrin carbons, suggesting that in the solid phase the kinetics of the migration of the central hydrogens is different than in solution.

Since it has been proposed that the origin of the pattern displayed by the pyrrole carbons in the CPMAS spectrum is due to the quenching of the N-H tautomerism, this spectrum may be expected to be similar to a solution one recorded in the slow exchange limit. The pyrrole zone of a spectrum recorded at -80 °C is shown in Figure 4C, where four peaks can be distinguished at 133.6, 138.3, 143.6, and 150.6 ppm. This pattern is qualitatively

**Table II.** <sup>13</sup>C NMR Chemical Shifts of OEP in the Solution and Solid-State Spectra

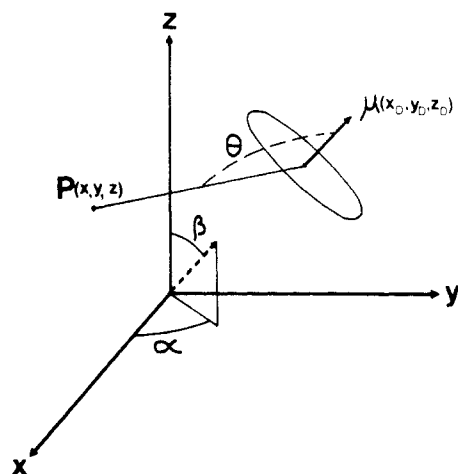
atom	chemical shift		
	solution (20 °C) <sup>a</sup>	solution (-80 °C) <sup>a</sup>	solid (30 °C) <sup>b</sup>
C <sub>α</sub> <sup>d</sup>		150.6	
	144.0 <sup>c</sup>		149.9, 137.0 <sup>f</sup>
C <sub>α</sub> <sup>e</sup>		133.6	
C <sub>β</sub> <sup>d</sup>		143.6	
	141.5		142.4, 137.0 <sup>f</sup>
C <sub>β</sub> <sup>e</sup>		138.3	
meso	96.5	95.8	95.0
CH <sub>2</sub>	20.0	19.0	19.4, 15.3
CH <sub>3</sub>	18.5	18.5	18.0, 16.0, 13.5

<sup>a</sup>In ppm downfield from TMS with CD<sub>2</sub>Cl<sub>2</sub> as solvent. <sup>b</sup>In ppm downfield from TMS with the CH<sub>3</sub> resonance of hexamethylbenzene as external reference. <sup>c</sup>Broad signal. <sup>d</sup>Carbons in the α-pyrroline-like ring (Figure 1). <sup>e</sup>Carbons in the (1*H*)-pyrrole-like ring. <sup>f</sup>Coalesced signals.

different from the one observed in the solid-state spectrum where three peaks appear at 137.0, 142.4, and 149.9 ppm implying that, unless severe solid-state effects other than kinetic ones are acting upon these carbons, the origin of the multiplicities in the observed signals should not be attributed to the presence of only one tautomer in solid OEP.

In order to distinguish the α from the β carbons in the -80 °C spectrum, spectra of OEP were recorded between this temperature and 20 °C. At -10 °C the α carbon peak cannot be distinguished any longer from the background noise, whereas the maximum width of the β carbons is achieved between -30 and -50 °C. However, at the latter temperature two peaks are detectable around 150.5 and 134 ppm, indicating that the N-H exchange has become slow on the NMR time scale for the α carbons. We therefore assign the peaks at 133.6 and 150.6 ppm in the -80 °C spectrum to the α carbons and the peaks at 138.3 and 143.6 ppm to the β carbons. As for TPrP, the high-field α-carbon resonance is assigned to the (1*H*)-pyrrole-like ring and the low-field one to the α-pyrroline-like ring. Although the lack of β hydrogens precludes an unambiguous assignment of the β carbons in OEP by the method described for TPrP, we will tentatively assign the high- and low-field β-carbon resonances to the (1*H*)-pyrrole-like and to the α-pyrroline-like ring, respectively. It will be shown below that this assignment, which is similar to that found for the β carbons of TPrP, will allow us to explain some fine structure details in the solid-state spectrum of OEP. It should be noticed that the assignment of the α and β carbons proposed here (and summarized in Table II) is different from the one suggested in the previous study of OEP.<sup>27</sup>

**Ring Current Effects.** A main drawback of the <sup>13</sup>C CPMAS technique is that the factors influencing the spectra are not always easy to isolate. Therefore, before analyzing the effects that the crystal packing may exert on the chemical exchange  $\mathbf{a} \rightleftharpoons \mathbf{b}$ , it may be interesting to focus attention on other solid-state effects that could influence the spectra of porphyrins. A possible mechanism that operates in the latter spectra but not in their solution counterparts is the shifts induced by the π aromatic clouds of neighboring molecules on the molecule under study. In solution NMR studies of porphyrins these aromatic ring currents are one of the determining factors in the chemical shifts of the protons. A method that has been proposed to evaluate the effects of these ring currents consists of replacing the π electron cloud by an equivalent dipole.<sup>36</sup> This approximation, in addition to being conceptually and computationally very simple, has generally given good results. Still a better approximation can be made for reproducing porphyrin ring currents if they are replaced by 16 equivalent dipoles, 8 above the macrocycle and 8 below it.<sup>37</sup> A suitable parametrization of this model allows a good fit (up to

**Figure 5.** General coordinate system suitable for evaluating intermolecular ring current shifts (see text).

0.1 ppm) between the calculated and the observed <sup>1</sup>H NMR chemical shifts of porphyrin protons,<sup>38</sup> of protons belonging to ligands axially bound in metalloporphyrins,<sup>39</sup> and of protons in aggregated porphyrins.<sup>40</sup> However, ring currents have not enjoyed the same popularity in <sup>13</sup>C NMR as in <sup>1</sup>H NMR, mainly due to the fact that predictions of ring current shifts in <sup>13</sup>C NMR spectra can seldom be checked experimentally. Since carbon chemical shifts are more sensitive to electronic and steric factors than protons, only in cases where these effects are the same in the molecule under study and in a suitably selected reference compound can ring current effects be checked.<sup>41</sup>

Intermolecular contacts between porphyrin molecules in the solid phase (~4 Å) are, due to the effective crystal packing, significantly smaller than those found for aggregated porphyrins in solution (~9 Å, see ref 40b). Therefore, it has been proposed<sup>27</sup> that ring current effects might be observed in the <sup>13</sup>C CPMAS spectra of porphyrins if a suitable reference compound can be chosen. In the cases under study, the molecule in solution can be taken as reference since no evidence of aggregation could be detected when recording 500-MHz <sup>1</sup>H NMR spectra of TPrP at different concentrations.

According to the 16-dipole model, the isotropic chemical shift ( $\delta$ ) due to the porphyrin ring currents at any point  $\vec{P} = (x, y, z)$  is given (in ppm) by

$$\delta(\vec{P}) = \mu_P \sum_i \frac{(1 - 3 \cos^2 \theta)}{r_{iP}^3} + \mu_H \sum_j \frac{(1 - 3 \cos^2 \theta)}{r_{jP}^3} \quad (1)$$

where  $\mu_P$  and  $\mu_H$  are constants proportional to the equivalent dipoles centered in two kinds of currents loops,  $r_{iP}$  is the distance between point  $\vec{P}$  and dipole  $i$ , and  $\cos \theta$  is the cosine of the angle between the equivalent dipole direction (perpendicular to the loop plane) and the direction associated with the vector connecting the equivalent dipole with point  $\vec{P}$ . If  $\mu_i$  is an equivalent dipole centered at  $(x_D, y_D, z_D)$  and with a direction given by the polar and azimuthal angles  $\alpha$  and  $\beta$ , then (see Figure 5)

$$\cos \theta_{iP} = [(\cos \beta)(z - z_D) + (\sin \beta \cos \alpha)(x - x_D) + (\sin \beta \sin \alpha)(y - y_D)] / [(z - z_D)^2 + (x - x_D)^2 + (y - y_D)^2]^{1/2} \quad (2)$$

In a recent application of this model to the interpretation of the <sup>13</sup>C CPMAS NMR spectrum of OEP, the equivalent dipoles  $\mu_H$  and  $\mu_P$  were varied until a good fit between a simulated

(38) Abraham, R. J.; Bedford, G. R.; Mc Neille, D.; Wright, B. *Org. Magn. Reson.* **1980**, *14*, 418.

(39) Abraham, R. J.; Medforth, C. J. *Magn. Reson. Chem.* **1987**, *25*, 432.

(40) (a) Abraham, R. J.; Smith, K. M.; Goff, D. A.; Bobe, F. W. *J. Am. Chem. Soc.* **1985**, *107*, 1085. (b) Katz, J. J.; Shipman, L. L.; Cotton, T. M.; Janson, T. R. in ref 11, Vol. 5, pp 402-458.

(41) Du Vernet, R.; Boekelheide, V. *Proc. Natl. Acad. Sci. U.S.A.* **1974**, *71*, 2961.

(36) Pople, J. A. *J. Chem. Phys.* **1956**, *24*, 1111.

(37) (a) Abraham, R. J.; Medforth, C. J.; Smith, K. M.; Goff, D. A.; Simpson, D. J. *J. Am. Chem. Soc.* **1987**, *109*, 4786. (b) Abraham, R. J.; Smith, K. M.; Goff, D. A.; Lai, J.-J. *J. Am. Chem. Soc.* **1982**, *104*, 4332.

spectrum and the recorded one was obtained.<sup>27</sup> However, it has been found by solution <sup>1</sup>H NMR that ring current shifts in porphyrins do not vary appreciably when changing the ring substituents from aromatic to aliphatic or even when quelling the macrocycle with a diamagnetic metal.<sup>38</sup> Hence, rather than vary  $\mu_H$  and  $\mu_P$ , we prefer to use the parameters obtained from <sup>1</sup>H NMR in order to find out what are the shifts that can be expected in the <sup>13</sup>C CPMAS NMR spectra of porphyrins due to intermolecular ring current effects ( $\mu_H = 19.1$ ;  $\mu_P = 17.3$ ). Both for TPrP and for OEP the calculations are based on the reported X-ray structure for these compounds.

TPrP crystallizes in space group  $P2_1/c$  and has two molecules per unit cell,<sup>29</sup> but ring current shifts only have to be evaluated on half a molecule due to symmetry considerations. The calculations took into account the effects of the 52 molecules in the 26 neighboring unit cells as well as the effects of the second molecule within the unit cell under study. It is convenient to analyze first the ring current effects on the meso and the alkyl chain carbons where the effects of the N-H chemical exchange process, if present, are expected to be very small. Calculated ring current shifts on meso carbons are -1.9 and -3.8 ppm, which should shift the solution peak observed at 118.7 ppm to two peaks centered at 114.9 and 116.8 ppm in the solid, in reasonable agreement with the values 115.0 and 116.7 ppm observed.<sup>42</sup> A similar analysis for the methylene carbons indicates that two peaks should appear at 14.7 and 13.2 ppm, close to the observed values of 15.3 and 13.6 ppm (Figure 2C). However, when the calculations are performed for the methylene carbons the observed spectrum is not correctly reproduced. Calculated ring current shifts are -3.5 and -1.2 ppm for methylenes  $\alpha$  to the macrocycle, and -1.3 and -1.1 for methylenes  $\beta$  to the macrocycle. These shifts combined with the solution  $\delta$  values predict three peaks in the CPMAS spectrum appearing at 36.5, 34.2, and 31.0 ppm with area ratios 1:1:2, whereas only two peaks are observed at 33.2 and 38.9 ppm with relative areas 3:1 (see above). This indicates that either the isotropic chemical shifts of the methylene carbons of an isolated TPrP molecule are different in solid and in solution or splitting mechanisms other than intermolecular ring current shieldings are operating on the methylene carbons of solid TPrP.

Ring currents also affect the resonance frequencies of the  $\alpha$  and  $\beta$  pyrrole carbons. For the (1*H*)-pyrrole-like ring, the double dipole model predicts shifts of -3.5 ppm for the  $\alpha$  carbons and -3.8 ppm for the  $\beta$  carbons. In the  $\alpha$ -pyrrolenine-like ring the  $\alpha$  carbons are shifted -1.7 ppm while the  $\beta$  carbons are not shifted on the average. Of course, these differences are too small to explain by themselves the doublings occurring in the pyrrole carbons region, but ignoring them could introduce errors when calculating the constants that control the hydrogen migration process. In the low-temperature solution <sup>13</sup>C NMR spectrum of TPrP, the  $\beta$  carbons appear at 125.0 and 131.7 ppm (splitting = 6.7 ppm), whereas in the CPMAS spectrum they appear at 121.0 and 130.8 ppm (splitting = 9.8 ppm). This difference in the splittings cannot be attributed to the intrinsic referencing inaccuracy of the solid-state technique, since it would equally affect both resonances. An explanation can, however, be based on intermolecular ring current effects. If the shifts predicted for the  $\beta$  carbons of the (1*H*)-pyrrole-like and of the  $\alpha$ -pyrrolenine-like ring by the double dipole model are added to the chemical shifts of the corresponding  $\beta$  carbons in solution, which have been identified by selective irradiation (see above), a "corrected" spectrum is obtained in which the  $\beta$  carbons appear at 121.2 and 131.6 ppm. In this case the difference between the  $\beta$  resonances is 10.4 ppm, in good agreement with the splitting observed in the solid state. The situation for the  $\alpha$  carbons is similar. Solution low-temperature chemical shifts of these carbons are 137.0 and 154.0 ppm. Adding to these values the ring current contributions

(42) It should be considered that the chemical shifts of the <sup>13</sup>C CPMAS NMR spectrum are exact within 2-3 ppm. This arises from the fact that an external reference is used, as well as due to the large line widths of the peaks (2-3 ppm). When evaluating ring current effects, interest should be placed on the magnitudes of the splittings rather than on the absolute chemical shifts values.

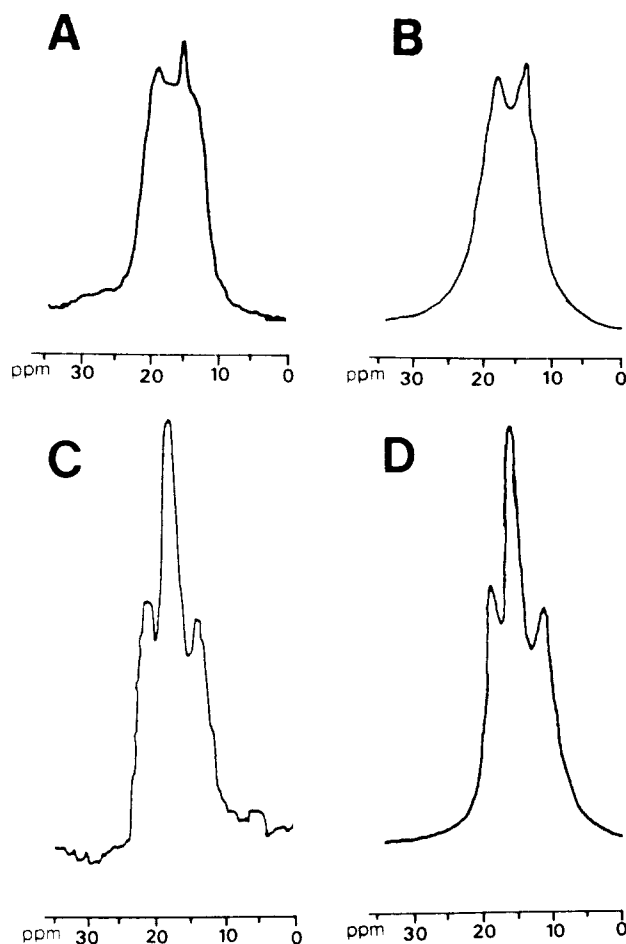


**Figure 6.** Experimental (A, C) and simulated (B, D) spectra of the ethyl carbons appearing in the <sup>13</sup>C CPMAS NMR spectrum of OEP. Spectrum A was recorded with a contact time of 40  $\mu$ s and shows only the methylene carbons. Spectrum C was recorded with a dipolar dephasing time of 50  $\mu$ s and shows only the methyl carbons. Other spectral parameters are the following: average number of scans = 35000, sweep width = 10000 Hz, line broadening = 0 Hz, repetition time = 2 s. Spectra were Fourier transformed with 4096 points. Simulations were performed as described in the text. Calculations predict four CH<sub>2</sub> carbons (B) appearing at 19.7, 18.9, 15.7, and 15.2 ppm; for the 15.7-ppm peak a line width of 70 Hz was used whereas a line width of 80 Hz was used for the rest of the methylene carbons. For the methyl carbons, calculations predict four unequivalent carbons appearing at 18.3, 16.7, 16.3, and 14.5 ppm; the 32-Hz line width was assumed for these carbons in order to perform the simulations.

gives two peaks at 133.5 and 152.3 ppm, very near the solid-state frequencies (134.0 and 152.5 ppm) for the  $\alpha$  carbons. These coincidences support not only the approach taken for calculating the ring current shifts but also the spectral assignments.

Ring current effects were also evaluated for OEP. Calculations were carried out on half a molecule due to the inversion center that these molecules possess in the solid state,<sup>28</sup> and the 26 nearest neighboring cells were taken into account. As for the TPrP case, it is more convenient to test the double dipole model in the meso and alkyl carbons. For the meso carbons, the calculations predict shifts of -0.9 and -2.6 ppm and although the resulting splitting is obscured by the natural line width of the resonances, it may be contributing to the observed width of the meso signal. A more interesting case can be found in the ethyl carbon resonances. Whereas in solution the CH<sub>3</sub> and CH<sub>2</sub> resonances are readily distinguishable, in the solid state they appear as a single peak of ca. 5 ppm half-width. Looking for fine structure within this broad resonance, the dipolar dephasing and the short contact time pulse sequences were employed. The resulting spectra of the methyl and methylene groups, together with those simulated by using the solution chemical shift values corrected by ring current effects, are shown in Figure 6. Both spectra were simulated with

moderate success, and an upfield shift in the CH<sub>2</sub> resonances that superimposes them on the CH<sub>3</sub> resonances can also be observed.

If at room temperature solid OEP would consist of only one tautomeric structure, it should be possible to obtain the pyrrole zone in the CPMAS spectrum by correcting the α and β carbon chemical shifts at -80 °C by the ring current effects and by taking into account the small temperature dependence of these resonances.<sup>43</sup> With use of the aforementioned assignments of OEP, four peaks should therefore appear at 133.6 and 151.4 ppm (α carbons, split = 17.8 ppm) and at 135.7 and 143.5 ppm (β carbons, split = 7.8 ppm). As can be appreciated in Figure 4, this is not coincident with the <sup>13</sup>C CPMAS NMR spectrum. It may be worthwhile to note that if the assignments of the α and β carbon resonances are reversed, the ring current shift corrections still fail to reproduce correctly the room temperature CPMAS spectrum.

**TPrP: Chemical Exchange.** In order to characterize properly the N-H tautomerization process of TPrP, a variable-temperature solid-state NMR analysis of this compound was performed. Since the strong overlapping of the pyrrole region in the full spectrum of TPrP complicated the analysis, spectra of TPrP were recorded by using the dipolar dephasing sequence or short contact times. As discussed above, intermolecular ring currents are an operating factor in the solid-state spectra of porphyrins. Therefore, the corrections described above for the room-temperature spectrum of TPrP due to these effects have to be taken into account at every temperature since the rate of hydrogen migration will affect the electronic environment of the pyrrole carbons, but not the through-space effects originating in neighboring molecules. Although crystal symmetry predicts up to four possible signals for each of the α and β carbons in the CPMAS spectrum, a simplification may be introduced by taking into account the fact that the calculated ring current effects for the α or the β carbons are similar within each five-membered ring. The problem can therefore be described as a superposition of two two-site systems, each possessing its own transverse relaxation time, its own equilibrium magnetization value *M*<sub>0</sub>, and two Larmor frequencies that are the low-temperature solution chemical shifts corrected by ring current effects. Both systems share the same exchange rates *k*<sub>ab</sub> and *k*<sub>ba</sub> and they behave approximately as predicted by the McConnell formalism.<sup>44</sup> The line widths used for each system were obtained from the low-temperature spectrum, but the variations of the cross polarization with temperature made it necessary to use different *M*<sub>0</sub> values at different temperatures.

In order to simulate the spectra two kinetic constants are required (*k*<sub>ab</sub> and *k*<sub>ba</sub>, see Figure 1), although it is also possible to use one kinetic constant and the equilibrium constant *K* = *k*<sub>ab</sub>/*k*<sub>ba</sub>. Both methods are equivalent, but the latter is more convenient since in the fast exchange limit the equilibrium constant can be directly extracted from the spectrum. For the α carbons, the position of the peaks in the high-temperature limit (fast exchange) is given by

$$\delta_1 = p_a \delta_{C_{\alpha}=\text{N}-} + p_b \delta_{C_{\alpha}\text{NH}-} + \delta_{1rc} \quad (3)$$

$$\delta_2 = p_a \delta_{C_{\alpha}\text{NH}-} + p_b \delta_{C_{\alpha}=\text{N}-} + \delta_{2rc} \quad (4)$$

where δ<sub>C<sub>α</sub>=N-</sub> and δ<sub>C<sub>α</sub>NH-</sub> are the solution chemical shifts in the α-pyrroline-like ring and in the (1*H*)-pyrrole-like ring, respectively, and δ<sub>1rc</sub>, δ<sub>2rc</sub> are the intermolecular ring current shifts on the α carbons of each ring (in this case, δ<sub>1rc</sub> = -1.7 ppm and δ<sub>2rc</sub> = -3.5 ppm if *p*<sub>a</sub> > *p*<sub>b</sub>). Since *p*<sub>a</sub> = 1/(1 + *K*) and *p*<sub>b</sub> = *K*/(1 + *K*), the difference δ<sub>1</sub> - δ<sub>2</sub> can be written as

$$\Delta = \delta_1 - \delta_2 = \Delta_0 \frac{(1 - K)}{(1 + K)} + \delta_{1rc} - \delta_{2rc} \quad (5)$$

(43) The assumption is made here that although the positions of the α and β carbon resonances in the <sup>13</sup>C NMR spectrum recorded at 20 °C do not coincide exactly with the centers of the α and β carbon doublets in the -80 °C spectrum (due to the temperature dependence of the chemical shifts), the splitting between the α and the β carbons in the two types of rings remains unchanged.

(44) McConnell, H. M. *J. Chem. Phys.* **1958**, *28*, 430. We shall disregard the effects introduced by the spinning of the sample.

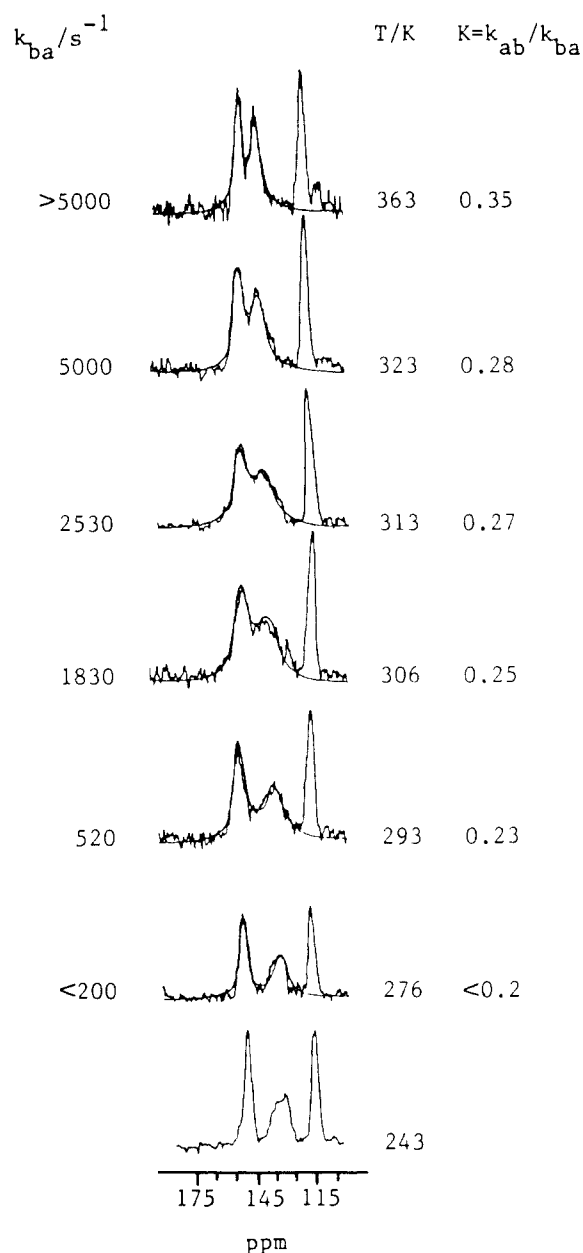


**Figure 7.** Superimposed experimental and calculated 25.16-MHz <sup>13</sup>C CPMAS spectra of the aromatic carbons of TPrP. Since the dipolar dephasing sequence was used, only the α and the meso carbons (115 ppm) appeared. 20000 scans were accumulated on the average; spectra were Fourier transformed with 4096 points and 10-Hz line broadening. The nonexchanging line widths (70 Hz and 150 Hz) were obtained from the low-temperature spectrum, where the effects of the coupling <sup>13</sup>C-<sup>14</sup>N are clearly visible.

where Δ<sub>0</sub> = δ<sub>C<sub>α</sub>=N-</sub> - δ<sub>C<sub>α</sub>NH-</sub> is the chemical shift difference in the solution low temperature spectrum. This allowed us to obtain the equilibrium constant *K* from the high-temperature spectra of the α and the β carbons, a value that was latter extrapolated to the intermediate exchange region assuming that *K* has an exponential temperature dependence *K* = *A* exp(-*E*/*RT*). The process **a** ⇌ **b** can then be analyzed by varying only the rate constant *k*<sub>ba</sub>. Experimental and calculated 25-MHz <sup>13</sup>C CPMAS NMR spectra of the α carbons as a function of temperature are shown in Figure 7, together with the rate constants of interconversion *k*<sub>ba</sub> and the equilibrium constants of the tautomerism used in the simulations. The spectra obtained for the β carbons at different temperatures can also be satisfactorily simulated by using the same approach as that described for the α carbons.

Up to this point, we have not explicitly considered the complications that may arise in the <sup>13</sup>C CPMAS NMR spectra of porphyrins by the presence of the nitrogen atoms. It is known<sup>45-49</sup>

that the eigenstates of the  $^{14}\text{N}$  nuclei are not in general eigenstates of the Zeeman Hamiltonian. This precludes the averaging of the dipolar coupling between neighboring  $^{13}\text{C}$ - $^{14}\text{N}$  nuclei by the magic-angle spinning, and the residual coupling may affect the shape of the  $\alpha$  carbon resonances. Although the dipolar Hamiltonian  $^{13}\text{C}$ - $^{14}\text{N}$  under MAS conditions has been solved exactly by numeric means, we prefer to use here a first-order perturbative approach that has been found to give satisfactory results for the observed spectra.<sup>49</sup> This approach predicts a split in the resonance of a carbon nucleus close to a  $^{14}\text{N}$  into two peaks of an area ratio 2:1. The magnitude of the splitting is given by

$$S = (9/20)(D\chi/Z_N)(3 \cos^2 \beta^D - 1 + \eta \sin^2 \beta^D \cos 2\alpha^D) \quad (6)$$

where  $\chi = e^2qQ/h$  is the  $^{14}\text{N}$  quadrupole coupling constant,  $\eta$  is the asymmetry parameter of the quadrupole tensor ( $\eta = (q_{xx} - q_{yy})/q_{zz}$ ),  $Z_N$  is the Larmor frequency of the  $^{14}\text{N}$  in the applied field,  $D = \gamma_C\gamma_N h/4\pi r^3$  is the dipolar coupling constant, and  $\beta^D$ ,  $\alpha^D$  are the polar and azimuthal angles that define the direction of the  $^{13}\text{C}$ - $^{14}\text{N}$  bond in the frame given by the principal axes of the quadrupole tensor ( $|q_{zz}| > |q_{yy}| > |q_{xx}|$ ). The splitting expected for the  $\alpha$  carbons (for the  $\beta$  carbons  $S \sim 0$  due to the  $r^{-3}$  factor) could be calculated if the NQR and the X-ray analyses of TPrP were available. Although to our knowledge the former has not been performed yet,  $^{14}\text{N}$  quadrupole parameters have recently been measured in the metastable triplet state of free base porphine via electron spin-echo envelope modulation.<sup>50</sup> In this study, the porphine guest was oriented in an *n*-octane host at 1.4 K; therefore allowing not only for the measurement of  $\chi$  and  $\eta$  but also for the orientation angles  $\beta^D$  and  $\alpha^D$  for each nitrogen. For the azine nitrogen, it was found that  $|\chi| = 3.317$ ,  $\eta = 0.165$ , the *z* axis of the quadrupole tensor points toward the *n* nitrogen orbitals, and the *x* axis is perpendicular to the porphyrin plane ( $\beta^D = 125^\circ$ ,  $\alpha^D = 90^\circ$ ). With these values, and the average C=N distance taken from the X-ray analysis (1.372 Å), eq 6 predicts for the  $\alpha$  carbons in the  $\alpha$ -pyrroline-like ring a split of 22 Hz. For the imino nitrogens, the values given by the spin-echo technique are  $|\chi| = 2.337$ ,  $\eta = 0.437$ ,  $\beta^D = 90^\circ$ ,  $\alpha^D = 125^\circ$ , while the X-ray diffraction study shows an average distance C-NH of 1.376 Å. Thus, the split observed for the  $\alpha$  carbons in the (1*H*)-pyrrole-like ring should be ca. -140 Hz. In the lowest temperature spectrum of TPrP (Figure 7, 243 K) where the  $\alpha$  carbons are no longer exchange broadened, it can be appreciated that the carbons of the (1*H*)-pyrrole-like ring (higher field signal) are considerably broader than those in the  $\alpha$ -pyrroline-like ring, in accordance with the results calculated with eq 6.<sup>51</sup> In the simulations of the higher temperature spectra, the effects of the nitrogens were implicitly taken into account by employing the line widths of the  $\alpha$  carbons that were measured at low temperature.

**OEP: Chemical Exchange.** Although the theoretical considerations involved in the study of the N-H tautomerization process

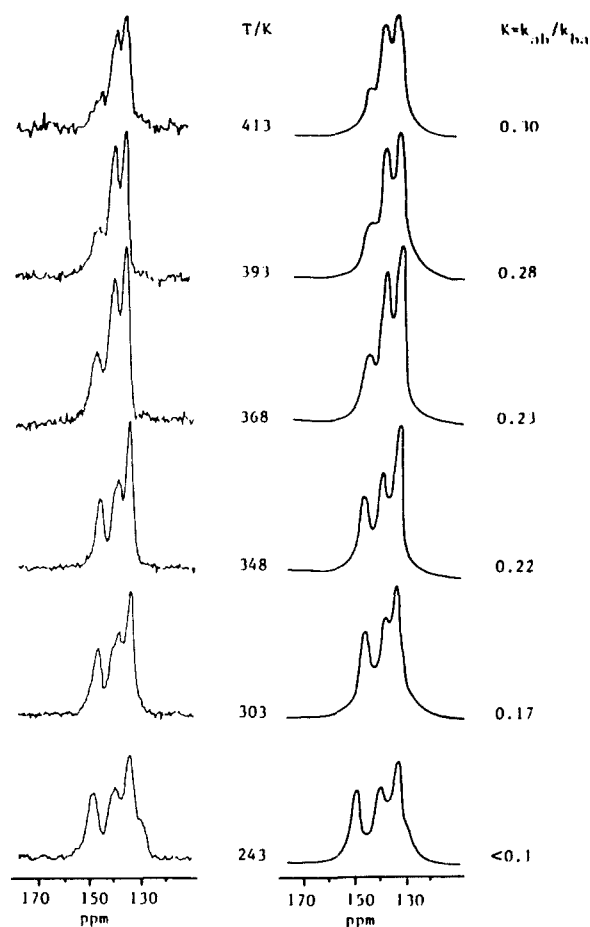


**Figure 8.** Experimental and calculated 25.16-MHz  $^{13}\text{C}$  CPMAS spectra of the  $\alpha$  and  $\beta$  carbons of OEP at different temperatures. Spectral conditions are similar to those described in Figure 7. A line width of 170 Hz was attributed to the  $\alpha$  carbon that is most affected by the coupling with the  $^{14}\text{N}$ ; a line width of 90.0 Hz was attributed to the other  $\alpha$  carbon signal as well as to the  $\beta$  carbons. Different equilibrium magnetization values  $M_0$  were attributed to the  $\alpha$  and to the  $\beta$  carbons, and the ratio  $M_0^\alpha/M_0^\beta$  was varied with the temperature from 0.4 (413 K) to 1.2 (243 K). All the spectra between 303 and 413 K were successfully simulated with use of a rate constant  $k_{ba} > 2000 \text{ s}^{-1}$ ; the spectrum at 243 K could be simulated by using a rate constant  $k_{ba} < 100 \text{ s}^{-1}$ .

in OEP and in TPrP are the same, the spectra of OEP are more difficult to analyze due to the severe peak overlap in the pyrrole carbon region. As mentioned above, the low-temperature solution spectrum does not resemble the room temperature solid state spectrum even after taking into account the ring current effects, since the splittings in the  $\alpha$  and  $\beta$  carbon resonances are smaller in the latter than in the former. Analysis of eq 5 indicates that this can be explained by assuming a tautomerization process occurring above the coalescence temperature between two unequally populated tautomers. In order to quantify the kinetic constants  $k_{ab}$  and  $k_{ba}$  involved in OEP N-H tautomerism, spectra were recorded between the slow and the fast exchange limits. As in the case of TPrP, each type of carbon ( $\alpha$  or  $\beta$ ) can be simulated by superimposing two two-site exchange processes. Experimental and calculated spectra of the pyrrole carbons at different temperatures are shown in Figure 8, together with the equilibrium constant  $K$  at each temperature. Differences in the heights and the areas of the  $\alpha$  and the  $\beta$  peaks, clearly visible at higher temperatures, can be attributed to cross polarization and  $^1\text{H}$  decoupling effects. The strong peak overlapping precluded the obtention of reliable rate constants at different temperatures, although in the 243 K spectrum the changes occurring when the reaction becomes slow on the NMR time scale are detected.

Once the equilibrium constants had been obtained at different temperatures, it was profitable to reexamine the room temperature spectrum of OEP. For the sake of simplicity we will assume that

(45) (a) Opella, S. J.; Hexem, J. G.; Frey, M. H.; Cross, T. A. *Phil. Trans. R. Soc. London, Ser. A* **1981**, 299, 665. (b) Hexem, J. G.; Frey, M. H.; Opella, S. J. *J. Am. Chem. Soc.* **1981**, 103, 224. (c) Hexem, J. G.; Frey, M. H.; Opella, S. J. *J. Chem. Phys.* **1982**, 77, 3847.

(46) (a) Groombridge, C. L.; Harris, R. K.; Packer, K. J.; Say, B. J.; Tanner, S. F. *J. Chem. Soc., Chem. Commun.* **1980**, 4, 174. (b) Harris, R. K.; Jonsen, P.; Packer, K. J. *Org. Magn. Reson.* **1984**, 22, 784. (c) Harris, R. K.; Jonsen, P.; Packer, K. J. *Magn. Reson. Chem.* **1985**, 23, 565. (d) Harris, R. K.; Jonsen, P.; Packer, K. J.; Campbell, C. D. *Magn. Reson. Chem.* **1986**, 24, 977.

(47) (a) Naito, A.; Ganapathy, S.; McDowell, C. A. *J. Chem. Phys.* **1981**, 74, 5393. (b) Naito, A.; Ganapathy, S.; McDowell, C. A. *J. Magn. Reson.* **1982**, 48, 367.

(48) Zumbulyadis, N.; Henrichs, P. M.; Young, R. H. *J. Chem. Phys.* **1981**, 75, 1603.

(49) (a) Olivieri, A. C.; Frydman, L.; Diaz, L. E. *J. Magn. Reson.* **1987**, 75, 50. (b) Olivieri, A. C.; Frydman, L.; Grasselli, M.; Diaz, L. E. *Magn. Reson. Chem.* **1988**, 26, 281.

(50) Singel, D. J.; Van der Poel, W. A. J. A.; Schmidt, J.; Van der Waals, J. H.; de Beer, R. J. *J. Chem. Phys.* **1984**, 81, 5453.

(51) The shape of the high-field  $\alpha$ -carbon resonance suggests that the larger peak of the doublet induced by the residual dipolar coupling is at higher fields than the smaller one. According to the convention used in the deduction of eq 6, this would be the case if  $\chi$  is negative, as was proposed in ref 50.



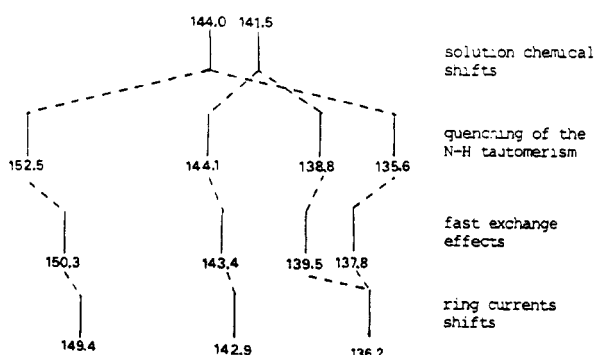


**Figure 9.** Diagram of the different factors that influence the spectral pattern of the pyrrole carbons of OEP in the solid state at room temperature. The solution spectrum consists of two peaks at 144.0 ppm ( $\alpha$  carbons) and 141.5 ppm ( $\beta$  carbons). If the N-H tautomerism would be quenched, four peaks would appear at 152.5, 144.1, 138.8, and 135.6 ppm. Since the reaction actually proceeds fast on the NMR time scale, the peaks move closer. The values shown in the figure can be obtained from eq 3-5 assuming an equilibrium constant  $K = 0.16$ . Finally, the intermolecular ring currents superpose the high-field signals ( $\alpha$  and  $\beta$  carbons in the (1*H*)-pyrrole-like ring), giving rise to a triplet with approximate relative heights 1:1:2.

the reaction is already in the fast exchange limit, where eq 3-5 are valid. The separation between the two  $\alpha$  carbon resonances is 12.9 ppm, smaller than the splitting between these carbons in the -80 °C solution spectrum of OEP ( $\Delta = 16.9$  ppm), while the splitting for the  $\beta$  carbons is 5.4 ppm, very similar to that found for these carbons in the solution spectrum of OEP at -80 °C ( $\Delta = 5.3$  ppm). The difference in the behavior of the  $\alpha$  and  $\beta$  carbons can be explained by taking into account the intermolecular ring current effects. Of all the porphyrin skeleton carbons, the double dipole model predicts that the most affected will be the two  $\beta$  carbons in the (1*H*)-pyrrole-like ring with an average high field shift of -3.3 ppm, whereas the other pair of  $\beta$  carbons will be shielded only by -0.8 ppm.<sup>52</sup> Hence, since the low-field  $\beta$ -carbon resonance was assigned to the latter nuclei, there will be an extra contribution of 2.5 ppm to the observed splitting for the  $\beta$  carbons in addition to the splitting that comes from the chemical exchange effects. Although these intermolecular shifts also affect the  $\alpha$  carbons, they do so to a smaller extent. The whole analysis for the pyrrole carbons of the room temperature spectrum of OEP is outlined in Figure 9. The coincidence that exists between the predicted and the observed spectrum not only justifies the assumption of taking ring current shifts as an operating mechanism in the solid-state spectra of porphyrins but also justifies the assignment of the high-field  $\beta$ -carbon resonance to the (1*H*)-pyrrole-like ring carbons, since a reversed assignment would not be able to explain the observed positions of the peaks.

**Discussion**

The tautomeric behavior of free base porphyrins is an excellent model for the analysis of a cyclic proton transfer process occurring between two covalently linked reactants. Moreover, the interest on this reaction has increased significantly since the discovery that free base phthalocyanine,<sup>53</sup> porphine,<sup>54</sup> and chlorin<sup>55</sup> are potential systems for performing data storage in the frequency domain (FDOS) by means of photochemical hole burning (PHB). This phenomenon is related to the phototautomerization that the central hydrogens undergo between two tautomers of unequal energies when they are placed in an inert matrix at cryogenic temperatures

**Table III.** Relevant Parameters for the N-H Tautomerism of TPrP and OEP in the Solid Phase

parameter	TPrP	OEP
$\Delta H$ (kcal/mol) <sup>a</sup>	1.3 ± 0.1	1.4 ± 0.1
$\Delta S$ (eu) <sup>a</sup>	1.4 ± 1	0 ± 1
$\Delta H^\ddagger$ (kcal/mol) <sup>b</sup>	12.8 ± 1	c
$\Delta S^\ddagger$ (eu) <sup>b</sup>	-2.2 ± 2	c

<sup>a</sup> From the equation  $K = k_{ab}/k_{ba} = e^{\Delta S/R} e^{-\Delta H/RT}$ . <sup>b</sup> From the equation  $k_{ba} = (kT/h) e^{\Delta S^\ddagger/R} e^{-\Delta H^\ddagger/RT}$ . <sup>c</sup> Not measured.

and are irradiated at a specific laser frequency. It has been shown that if appropriate systems are found, the presence or absence of a spectral hole at a particular frequency could be utilized to encode as many as 1000 or more bits in the frequency domain within a single focused laser spot.<sup>56</sup> The first observation of the N-H tautomerism by <sup>1</sup>H NMR was made 20 years ago, and during 15 years quantitative kinetic measurements have been focused mostly on tetraarylporphyrins. As a result of these studies, it has been established that the reaction is mainly intramolecular, with a kinetic behavior that is independent of the nitrogen basicities and of solvent effects. Kinetic isotope effects arising from the replacement of the central hydrogens by deuterons are also available. In addition, theoretical studies have been carried out,<sup>57-60</sup> drawing attention mainly on two points: the synchronicity of the hydrogens motion and the coupling between the porphyrin skeleton and the proton rearrangement. These studies indicated that either an asynchronous transfer process<sup>58,59</sup> or a skeletal deformation accompanying the migration<sup>59,60</sup> would reduce the activation energy of the process. However, the reliability of these calculations has been questioned<sup>61</sup> on the basis of the disagreement between the value of the barrier height predicted by the purely quantum mechanical calculations (~2.5 eV) and that measured by <sup>1</sup>H NMR (~0.45 eV). Although it is possible to reconcile the theoretical calculations with the experimentally measured barrier height by assuming the existence of a tunneling contribution to the reaction, certain facts indicate that such a contribution is unlikely.<sup>20,21</sup>

In order to gain more information about the aforementioned molecular details of the reaction, other free base porphyrin systems are being analyzed. One approach to the problem is to perturb the symmetry of tetraarylporphyrin systems by introducing different substituents in the  $\beta$  position of one pyrrole ring<sup>21</sup> thereby breaking the degeneracy of the tautomers. <sup>1</sup>H NMR allowed the measurement of two energy barriers for these compounds, as well as the notation of a remarkable directionality in the hydrogen transfer process. An alternative approach is based on the evaluation of the kinetic solid state effects acting on symmetrically substituted porphyrins applying the CPMAS NMR techniques either to isotopically enriched<sup>24,26</sup> or to natural abundance<sup>25</sup> compounds. As discussed in Results, evaluation of <sup>13</sup>C CPMAS NMR data and comparison with solution values are not straightforward. A main disadvantage of the solid-state technique as compared with solution <sup>1</sup>H dynamic NMR analyses is its lack of quantitiveness, as well as the presence of sometimes unpredictable factors that may affect the line widths or multiplicities of the signals. However, we have shown that by making some reasonable assumptions, energetic parameters involved in the solid-phase reaction can be obtained (Table III).

The perturbations occurring in the N-H transfer process of free base porphyrins are likely to be caused by the crystal packing effects of the lattice. As suggested in our previous work,<sup>25</sup> these effects may operate by two different mechanisms depending on whether or not the hydrogen migration is significantly coupled to a skeletal rearrangement. If it is assumed that tautomerism

(52) Since at room temperature tautomerism in OEP is no longer quenched, it is not strictly correct to talk about signals arising from the (1*H*)-pyrrole-like and  $\alpha$ -pyrroline-like rings. However, since in the solid state one tautomer is favored over the other (for example  $p_a > p_b$ ) we will continue to use these denominations.

(53) Romagnoli, M.; Moerner, W. E.; Schellenberg, F. M.; Levenson, M. D.; Bjorklund, G. C. *J. Opt. Soc. Am. B* **1984**, *341*, 1.

(54) Rebane, L.; Gorokhovskii, A. A.; Kikas, J. V. *Appl. Phys. B* **1982**, *29*, 235.

(55) Volker, S.; Macfarlane, R. M. *J. Chem. Phys.* **1980**, *73*, 4476.

(56) de Vries, H.; Wiersma, D. A. *J. Chem. Phys.* **1980**, *72*, 1851.

(57) Almlof, J. *Int. J. Quantum Chem.* **1974**, *8*, 915.

(58) Kuzmitzky, V. A.; Solovoyov, K. N. *J. Mol. Struct.* **1980**, *65*, 219.

(59) (a) Sarai, A. *Chem. Phys. Lett.* **1981**, *83*, 50. (b) Sarai, A. *J. Chem. Phys.* **1982**, *76*, 5554.

(60) Bersuker, G. I.; Polinger, V. Z. *Chem. Phys.* **1984**, *86*, 57.

(61) (a) Sarai, A. *J. Chem. Phys.* **1984**, *80*, 5341. (b) Limbach, H.-H. *J. Chem. Phys.* **1984**, *80*, 5343.

may proceed without a skeletal rearrangement, the perturbations of the solid-state reaction will depend on the static configuration that crystal packing forces induce on the porphyrin molecules. If tautomerism requires a skeletal rearrangement<sup>59</sup> then the crystal packing forces may perturb the reaction by precluding the rearrangement, favoring thereby the presence of one tautomer over the other.

As mentioned in the Introduction, high-resolution <sup>13</sup>C NMR is a sensitive tool for probing the structure of organic molecules. Therefore, its extension to the solid state allows the evaluation of extra electronic effects that originate in the crystal packing forces. As we have shown, the chemical shifts of TPrP and OEP in the slow exchange limit are not the same when the molecules are in the solid state as when they are in solution; but these differences may be understood in terms of intermolecular ring current effects without a need to invoke electronic effects. Thus, even though TPrP and OEP molecules in the solid state are distorted, this distortion is not large enough to be reflected on either the  $\alpha$ ,  $\beta$ , or meso carbons chemical shifts. It is not likely that such small distortions could account by themselves for the kinetic and thermodynamic perturbations that affect the N-H tautomerism when going from solution to the solid state.

If it is assumed that the proton transfer process is coupled to a skeletal rearrangement of the porphyrin macrocycle, a new theoretical approach to the problem is possible. When a rearrangement takes place in a crystal, the associated energy of the reaction or of the transition state is the sum of an intermolecular and of an intramolecular contribution. Until now, the main goal of the quantum mechanical calculations performed on free base porphyrins was the computation of the intramolecular contribution, and although many useful conclusions were reached, the figures obtained for the barrier height of the reaction did not follow those measured experimentally. An approach for the interpretation of the solid-state reactivity is to consider the energy profile of the hydrogen transfer in solid porphyrins (Table III, and ref 24-26) as a sum of a solution contribution (a symmetrical double minimum potential) plus the contribution of the packing energy at each point of the reaction coordinate. Since the time-averaged positions of the atoms in crystalline TPrP and OEP are known in full detail from the X-ray diffraction studies, a model might be proposed in which the molecule under study rearranges in an average crystalline potential field in such a way that the changes in potential packing energy reproduce satisfactorily the intermolecular energy contribution measured by CPMAS NMR. These changes in the intermolecular energy, that result from electrostatic and nonbonded interactions, can be calculated by using methods reported in the literature.<sup>62</sup> Such calculations may help to resolve some of the many puzzles put forward by the tautomerism of free base porphyrins.

The CPMAS NMR technique has been used to examine N-H tautomerism in five free base porphyrins, namely, H<sub>2</sub>P, TPP, TPrP, OEP, and TTP. In every case it afforded evidence for the presence of more than one tautomer in the solid. With the exception of TTP, available X-ray data for these porphyrins<sup>27,28,63</sup> favor a static picture in which a pair of diagonally positioned pyrrole rings carry the hydrogens. The new kinetic and thermodynamic data that were obtained from the NMR studies suggest that a new look at the X-ray results might be profitable. The latter show that no symmetry is present in H<sub>2</sub>P molecules in the solid state, whereas a center of inversion is present in TPrP, TPP, OEP, and TTP. Nevertheless, all these porphyrins undergo N-H tautomerism in the solid, with equilibrium constants *K* ranging from 0.1 to 1. No apparent correlation can be found between the symmetry of the porphyrin macrocycle and N-H tautomerism. Therefore, the requirement of tetragonal symmetry to ensure this type of dynamic disorder does not appear to be as necessary as previously suggested.<sup>64</sup>

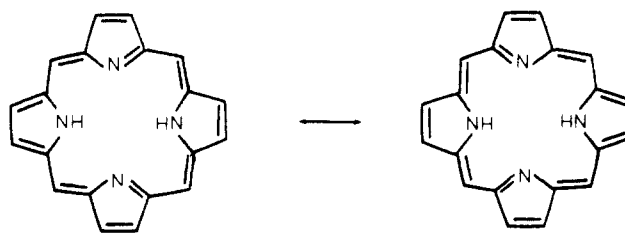


**Figure 10.** Canonical resonance structures of one of the tautomers shown in Figure 1. The single and double character of the bonds would explain the deformations of the porphyrin macrocycle when the hydrogens are localized in one pair of opposite pyrrole rings.

It also may be convenient to revisit the "common" structure that has been proposed for the skeleton of free base porphyrins.<sup>65</sup> When the first X-ray analyses of symmetrically substituted porphyrins were performed, it was recognized that these compounds were restricted to some class of 2-fold symmetry in the solid. Since the central hydrogens were localized in one pair of opposite pyrrole rings, the geometry in the solid was assumed to reflect the mean structure that the resonance hybrid shown in Figure 10 could adopt. For example, the C<sub>β</sub>-C<sub>β</sub> bonds in the  $\alpha$ -pyrroline-like rings are double bonds in both resonance structures, while in the (1*H*)-pyrrole-like ring they are double bonds in one structure but single bonds in the other, and this trend has indeed been found in the C<sub>β</sub>-C<sub>β</sub> bond lengths. Similar correlations were found for other distances (C<sub>α</sub>-C<sub>β</sub>, C<sub>α</sub>-N, etc.), as well as for the bond angles. Of all the differences between the (1*H*)-pyrrole-like and the  $\alpha$ -pyrroline-like rings in free base porphyrins, it has been predicted that the most significant ones should be found in the C<sub>α</sub>-N-C<sub>α</sub> bond angles (Figure 3 in ref 59b), a fact that has also been checked experimentally (Table VII in ref 28). However, the differences in these angles between the two types of pyrrole rings decrease in the order OEP (3.9°) > TPrP (3.4°) > TPP (3.0°) > H<sub>2</sub>P (2.5°) > TTP (0.5°), showing no correlation with the proportions between the tautomer populations found in the solid (Table III and ref 24-26). Further experimental work involving low-temperature X-ray diffraction and neutron scattering techniques may still be necessary to fully understand the structure-reactivity relationships that control the N-H tautomerism in solid free base porphyrins.

## Conclusions

The N-H tautomerism of TPrP and OEP was studied by high-resolution <sup>13</sup>C NMR in the solid state and in solution. The spectra of TPrP could be completely assigned using selective irradiation in solution and the dipolar dephasing technique in the solid state. Differences between the solution and the solid-state chemical shifts of the pyrrole carbons were satisfactorily explained invoking intermolecular ring current effects. Simulations of the spectra of TPrP at different temperatures were successfully performed using the splittings in the low temperature solution spectrum as well as the shifts given by the 16-dipole method with the original parametrization. The effects of the <sup>14</sup>N nuclei on the  $\alpha$  carbons were also observed in the -30 °C solid state spectrum of TPrP and were rationalized by using a first-order perturbative approach and literature values of the quadrupole parameters found for porphine in the excited triplet state. Ring-current effects could also account for other anomalies in the <sup>13</sup>C CPMAS spectrum of TPrP shown by the non-pyrrolic carbon resonances. Spectra of OEP were recorded at different temperatures and indicated that, contrary to what has been previously proposed, the N-H tautomerization process was not quenched at room temperature. Although the absence of  $\beta$  hydrogens precluded any simplification in the pyrrole carbon region of the CPMAS spectra, the N-H exchange could be partially analyzed in the range from slow to fast exchange. Ring-current effects were also used to understand the room temperature spectrum and helped to assign the origin of each  $\beta$  carbon resonance. A method that could be used to

(62) (a) Gavezzotti, A.; Simonetta, M. *Chem. Rev.* **1982**, *82*, 1. (b) Dauber, P.; Hagler, A. T. *Acc. Chem. Res.* **1980**, *13*, 105.

(63) (a) Silvers, S. J.; Tulinsky, A. *J. Am. Chem. Soc.* **1967**, *89*, 3331. (b) Chen, B. M. L.; Tulinsky, A. *J. Am. Chem. Soc.* **1972**, *94*, 4144. (c) Butcher, R. J.; Jameson, G. B.; Storm, C. B. *J. Am. Chem. Soc.* **1985**, *107*, 2978.

(64) Hoard, J. L. in ref 12, Chapter 8, p 336 and ff.

(65) Tulinsky, A. *Ann. N.Y. Acad. Sci.* **1973**, *206*, 47 and ff.

explain the solid state effects shown by free base porphyrins is proposed, which takes into account possible rearrangements of porphyrin molecules in the crystal. Should these calculations give positive results, general conclusions could be drawn about porphyrin tautomerism.

The solid-state NMR results presented in this work do not appear to be in complete agreement with the previous X-ray analyses of the studied porphyrins. Although it is conceivable that the crystalline forms that we have employed for the CPMAS study are not the same as those used for the crystallographic analysis, it may be worthwhile to note that since hydrogen atoms are weak X-ray scatterers it is difficult to locate them by X-ray diffraction. This problem is highlighted when hydrogens are bonded to electronegative atoms like nitrogen, due to the distortion of the electron density along the N-H direction.<sup>66</sup> However, in the case of porphine (where  $K = 1$ ) it is possible to reconcile the presence of the two tautomers in the solid with the localization of the central hydrogens proposed by the X-ray analysis, if it is assumed that the tautomeric process is coupled to a rotation of

the molecule as a whole in such a way that the translational symmetry of the crystal is maintained. This could be achieved by a rotation of 90° about the main molecular axis combined with the hydrogen migration process. We are currently studying this possibility using wide line spectroscopy. In any case, we have shown that <sup>13</sup>C CPMAS NMR, when performed at different temperatures and corrected by intermolecular effects, is one of the most useful tools for studying dynamical processes in the solid state.

**Acknowledgment.** This research was supported by the National Institutes of Health under Grant GM 11973. Support by the Consejo Nacional de Investigaciones Cientificas y Tecnicas (CONICET) is also gratefully acknowledged. We thank Prof. David M. Grant and Charles L. Mayne (University of Utah) for help in recording the solution spectra within the frame of a NSF-CONICET binational grant. We are also grateful to Prof. Raymond J. Abraham (University of Liverpool) for discussions on ring current effects.

**Registry No.** TPrP, 22112-75-0; OEP, 2683-82-1; pyrrole, 109-97-7; butyraldehyde, 123-72-8.

(66) Taylor, R.; Kennard, O. *Acc. Chem. Res.* 1984, 17, 320.

## Indirect Two-Dimensional Heteronuclear NMR Spectroscopy. (<sup>31</sup>P, <sup>57</sup>Fe) Spectra of Organoiron Complexes

Reinhard Benn,\* Herbert Brenneke, Albert Frings, Herbert Lehmkuhl, Gerlinde Mehler, Anna Ruffińska, and Thomas Wildt

Contribution from the Max-Planck-Institut für Kohlenforschung, Kaiser-Wilhelm-Platz 1, D-4330 Mülheim a.d. Ruhr, Germany. Received December 14, 1987

**Abstract:** The indirect heteronuclear two-dimensional (2D) triple-resonance (S,I)-{<sup>1</sup>H} NMR spectroscopy is introduced for measuring the chemical shift and scalar spin-spin coupling constants of an insensitive nucleus I via its scalar coupling  $J(S,I)$  by detection of the nucleus S of higher sensitivity. The versatility of this approach is demonstrated by extracting  $\delta(^{57}\text{Fe})$  and  $J(\text{Fe},\text{X})$  from (<sup>31</sup>P,<sup>57</sup>Fe)-{<sup>1</sup>H} spectra of various dissolved  $[(\eta^5\text{-Cp})(\text{L}_2)(\text{R})]\text{Fe}$ ,  $[(\eta^3\text{-allyl})(\eta^5\text{-Cp})(\text{L})]\text{Fe}$ , and  $[(\eta^1,\eta^2\text{-alkenyl})(\eta^5\text{-Cp})(\text{L})]\text{Fe}$  complexes (R = alkyl, hydride; L = PR<sub>3</sub>). In practice the sensitivity of 2D (<sup>31</sup>P,<sup>57</sup>Fe) spectra was found to be higher than that of the direct observation scheme by at least a factor  $(\gamma_{\text{P}}/\gamma_{\text{Fe}})^{5/2}$ . At 9.4 T typical recording times for 5-mm samples of low concentration (1-5%, v/v) are of the order of 1 h. Thus, the iron NMR parameters of many complexes become accessible in the most effective manner when the indirect (<sup>31</sup>P,<sup>57</sup>Fe) recording scheme is used. Due to the intrinsically higher resolving power of a two-dimensional experiment, small scalar couplings like <sup>2</sup>J(Fe,F) and <sup>1</sup>J(Fe,H) were readily obtained from indirect two-dimensional spectra. Combinations of (<sup>1</sup>H,<sup>57</sup>Fe) and (<sup>31</sup>P,<sup>57</sup>Fe) spectra yielded the relative signs of the  $J(\text{Fe},\text{X})$  couplings: <sup>1</sup>J(Fe,P) is positive and increases with increasing  $\pi$ -acceptor power of the phosphorus ligand L from 55 (L = PMe<sub>3</sub>, R = H) to 149 Hz (L = PF<sub>3</sub>). <sup>1</sup>J(Fe,H) is around +9 Hz (R = H), whereas <sup>2</sup>J(P,H) in these complexes was found to be negative. In all of the allyl complexes investigated, <sup>2</sup>J(Fe,F) (L = PF<sub>3</sub>) is positive and around 3 Hz. In the quasi-tetragonal and -trigonal iron complexes,  $\delta(^{57}\text{Fe})$  varies by about 4000 ppm. This can be rationalized qualitatively by the electronegativity of the atoms directly bonded to iron and the higher oxidation potential in the presence of more basic ligands L via the paramagnetic shielding term.

Complexes of iron play an important role in inorganic<sup>1</sup> and organometallic<sup>2</sup> chemistry as well in a variety of industrial processes<sup>3</sup> and biological systems.<sup>4</sup> The number of <sup>57</sup>Fe NMR studies of dissolved complexes,<sup>5</sup> however, is still limited,<sup>6-8</sup> and, conse-

quently, the total range of the <sup>57</sup>Fe shift scale is unknown. Only a few indirect scalar spin-spin couplings  $J(\text{Fe},\text{X})$  (e.g. X = <sup>1</sup>H,<sup>9</sup> <sup>13</sup>C,<sup>10</sup> <sup>15</sup>N,<sup>11</sup> and <sup>31</sup>P<sup>7,9,10d,12</sup>) have yet been reported. This is because the <sup>57</sup>Fe nucleus is one of the most insensitive nuclei in NMR spectroscopy, and the natural abundance of magnetically active iron is only 2.19%.<sup>6-8</sup> Several approaches have been made to improve the recording conditions for this nucleus. Examples are steady-state pulse techniques,<sup>13</sup> the use of high magnetic fields,

(1) Cotton, F. A.; Wilkinson, G. *Advanced Inorganic Chemistry*; Wiley: New York, 1980; p 765.

(2) Koerner von Gustorf, E. A.; Grevels, F.-W.; Fischler, T. *The Organic Chemistry of Iron*; Academic: New York: 1978, Vol. 1; 1981, Vol. 2. Wilkinson, G., Stone, F. G. A., Abel, E. W., Eds. *Comprehensive Organometallic Chemistry*; Pergamon: Oxford, 1982; Vol. 4, p 243; Vol. 8, p 939.

(3) Weissermel, K.; Arpe, H. J. *Industrielle Organische Chemie*; Verlag Chemie: Weinheim, FRG, 1978.

(4) Lee, H. C.; Gard, J. K.; Brown, T. L.; Oldfield, E. J. *J. Am. Chem. Soc.* 1985, 107, 4087; Nozawa, I.; Sato, M.; Hatano, M.; Kobayashi, N.; Osa, T. *Chem. Lett.* 1983, 1289.

(5) To the best of our knowledge, solid-state <sup>57</sup>Fe NMR studies have not been reported until now.

(6) Dechter, J. J. *Prog. Inorg. Chem.* 1985, 33, 393.

(7) Philipsborn, W. v. *Pure Appl. Chem.* 1986, 58, 513.

(8) Benn, R.; Ruffińska, A. *Angew. Chem.* 1986, 98, 851.

(9) Benn, R.; Brevard, C. *J. Am. Chem. Soc.* 1986, 108, 5622.

(10) (a) Koridze, A. A.; Petrovskii, P. V.; Gubin, S. P.; Fedin, E. I. *J. Organomet. Chem.* 1975, 93, C26. (b) Koridze, A. A.; Astakhova, N. M.; Petrovskii, P. V. *Izv. Akad. Nauk SSSR, Ser. Khim.* 1982, 956; 1982, 957. (c) Jenny, T.; Philipsborn, W. v.; Kronenbitter, J.; Schwenk, A. *J. Organomet. Chem.* 1981, 205, 211. (d) Mann, B. E. *J. Chem. Soc., Chem. Commun.* 1971, 1173.

(11) Morishima, I.; Inubushi, T. *J. Chem. Soc., Chem. Commun.* 1978, 106.

(12) Brevard, C.; Schimpf, R. *J. Magn. Reson.* 1982, 47, 528.